Effect of Aging Treatment on Ultra-Fine Grains and Si-Phase in Al-0.5%Si Alloy Fabricated by ARB Process

AUTHOR(S):

Nakagawa, Keiyu; Kanadani, Teruto; Tsuji, Nobuhiro; Terada, Daisuke; Masui, Toshiaki; Sato, Yasuhiko

CITATION:

Nakagawa, Keiyu ...[et al]. Effect of Aging Treatment on Ultra-Fine Grains and Si-Phase in Al-0.5%Si Alloy Fabricated by ARB Process. Materials transactions 2011, 52(10): 1853-1859

ISSUE DATE:

2011-10

URL:

http://hdl.handle.net/2433/171915

Materials Transactions, Vol. 52, No. 10 (2011) pp. 1853 to 1859

Effect of Aging Treatment on Ultra-Fine Grains and Si-Phase in Al-0.5%Si Alloy Fabricated by ARB Process*[1]

Keiyu Nakagawa[1,*2], Teruto Kanadani[1], Nobuhiro Tsuji[2], Daisuke Terada[2], Toshiaki Masui[3] and Yasuhiko Sato[4]

[1]*Faculty of Engineering, Okayama University of Science, Okayama 700-0005, Japan*
[2]*Graduate School of Engineering, Department of Materials Science and Engineering, Kyoto University, Kyoto 606-8501, Japan*
[3]*Graduate School of Engineering, Osaka University, Suita 565-0871, Japan*
[4]*Graduate School of Engineering, Okayama University of Science, Okayama 700-0005, Japan*

Using TEM observation and Vickers micro-hardness measurements, this study investigated microstructural changes resulting from aging treatment of ultrafine-grained (UFG) Al-0.5%Si alloy fabricated with a six-cycle accumulative roll-bonding (ARB) process, which includes severe plastic deformation. Results show that the mean grain size of the UFGed Al-0.5%Si alloy produced by the ARB was 253 nm. The hardness of specimens aged at 373 K and 423 K decreased monotonously with increasing aging time in the initial stage of aging. The hardness value of the specimen aged at 373 K then became higher than the value of the specimen aged at 423 K after 10 ks. TEM observation revealed that the mean grain size of the UFG specimen aged at 373 K was less than that of the specimen aged at 423 K. Moreover, results confirmed that Si phase precipitates on the {111} planes on the matrix in the UFG specimen aged at 373 K and 423 K. The mean size of Si-phase in the UFG increased with aging time. The Si phase formation in the UFG specimen aged at 373 K is less than that of 423 K in long-term aging. However, the formation of Si phase on the grain boundaries is more conspicuous than in UFG specimens aged at 373 K and 423 K. These results suggest that restraint of the growth of UFG with aging resulted from Si phase precipitation on the grain boundary and lowering of the aging temperature. Moreover the formation of Si-phase in the UFG suggests precipitation hardening in the ARB-processed Al-Si alloy.
[doi:10.2320/matertrans.L-M2011819]

(Received October 1, 2010; Accepted June 15, 2011; Published August 31, 2011)

Keywords: *aluminum-0.5%silicon alloy, ultrafine grain, accumulative roll-bonding (ARB) process, silicon phase, precipitation hardening*

1. Introduction

Recently, the manufacture of aluminum alloys with ultrafine grains (UFG) of less than 1 µm mean size has become possible through severe plastic deformation,[1)] which includes high strain up to an equivalent strain of 4–5. UFG aluminum alloys obtained using severe plastic deformation exhibit surprisingly high strength that is 2–4 times higher than that of conventional coarse-grained materials. Such high strength is explained by the strength attributable to grain refinement. However, it is expected that they would show different aging behaviors from those of conventional coarse-grained materials because UFG aluminum alloys are full of grain boundaries.

Numerous previous studies of UFG aluminum alloys have assessed their mechanical properties, but few have examined aging behavior.[2,3)] Tsuji *et al.* described aging behavior of UFGed Al-2 mass%Cu alloy fabricated through accumulative roll-bonding (ARB).[2)] They concluded that hardness of the ARB processed alloy decreased monotonously during aging; no precipitation hardening was detected because of the lack of fine and coherent precipitates in UFG. Many grain boundaries act as nucleation sites and paths for the high-speed diffusion of solute atoms in UFG aluminum alloys that takes place through severe plastic deformation. Therefore, grain boundary precipitation is accelerated in UFG aluminum alloys. In addition, enhanced precipitation on the grain boundary is thought to reduce the concentration of super-saturated solute atoms in the UFG. Horita *et al.* reported grain precipitation achieved even inside the UFGed microstructure of an Al-10.8%Ag alloy fabricated using the equal channel angular pressing (ECAP) process.[3)] It is noteworthy that grain precipitation was observed at temperatures much lower than the conventional aging temperature range. Generally, Al-Si system alloys are precipitation-hardened aluminum alloys. The Si phase is precipitated finely in the specimen[4–6)] when a specimen of an Al-Si alloy is aged at a high temperature of about 473 K. In earlier studies, the authors investigated the formation of Si phase on the precipitation process in an Al-1.2% Si alloy by TEM observation, and it has been concluded that a plate-like Si-phase precipitate existed on the {111} plane at the initial stage of several tens of seconds of the precipitation process.[7)] Subsequently, the thickness and length of the plate-like Si phase increased with increasing aging time. The Si-phase precipitated finely on the {111}, {100}, and {110} plane in the specimen, and mean size and number density of Si-phase are inferred as main factors for precipitation-hardening in this alloy. The microstructural changes that occur with aging of UFGed Al-0.5% Si alloy were investigated to clarify the aging behavior of this alloy.

2. Experimental Methods

2.1 Specimens

The Al-0.5%Si alloy ingots were cast by melting 99.99%Al and 99.999% Si in air in a high-purity alumina crucible. The obtained ingots were homogenized. Their surface was peeled mechanically. They were then hot forged and cold rolled to produce 1 mm thick sheets for ARB. The 1 mm thick sheets were cut to 30 mm wide and 300 mm long

*[1]The Paper Contains Partial Overlap with the ICAA12 Proceedings by USB under the Permission of the Editorial Committee.
*[2]Corresponding author, E-mail: nakagawa@mech.ous.ac.jp

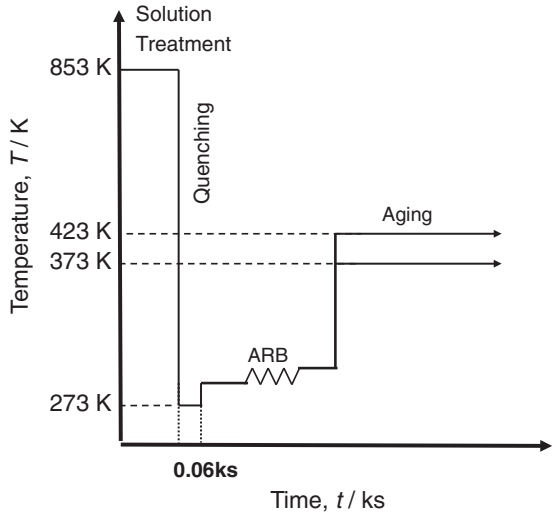

Fig. 1 Sequence of heat treatment for ARB-processed specimen.

pieces. Then they were processed using ARB. One side of the sheet surface was degreased using acetone and wire-brushed using steel wire. After the surface treatment, two sheet pieces were stacked so that the brushed surfaces were in contact and were fixed tightly together using stainless steel wire. Roll bonding was conducted with reduction in the thickness per cycle of 50% (equivalent strain, $\varepsilon = 0.8$/cycle). A rolling mill was used for roll bonding with reduction of 50% in one pass with lubrication. All procedures described above were conducted at room temperature.

2.2 Heat treatment

A schematic summary of the heat treatment schedule used in this work is presented in Fig. 1. Heat treatment as a solution heat treatment was performed at 853 K (T_Q) for 1.8 ks with subsequent quenching in ice water. Next, the specimens were pre-aged in an ice-water bath for 60 s and final aged for various durations (t_A) in a silicone oil bath held at 373 K or 423 K (T_A). The accuracy of T_A was ± 0.5 K. After aging treatment, the specimens were stored in liquid nitrogen.

2.3 Vickers hardness tests

For Vickers hardness tests, 30 mm × 10 mm × 1 mm sheets were cut from strips 1 mm thick. The surfaces of these sheets were polished using sandpaper and then electro-polished to prepare 0.9 mm thick specimens. The hardness of specimen was measured at room temperature using a Vickers micro-hardness tester (Akashi Corp.). Hardness was measured using a load of 0.48 N, and holding time was 20 s.

2.4 TEM observations

The ARB processed sheets' microstructures were observed by a transmission electron microscope (TEM, 2000EX; JEOL) operated at 200 kV to determine the detailed morphologies of matrix grains. Thin foils for TEM observation, which were perpendicular to the transverse direction (TD) of the sheets, were prepared using twin-jet electro-polishing in a 400 ml HNO_3 +500 ml CH_3OH +100 ml H_2O solution at −15°C. Microstructural observations of the precipitates at

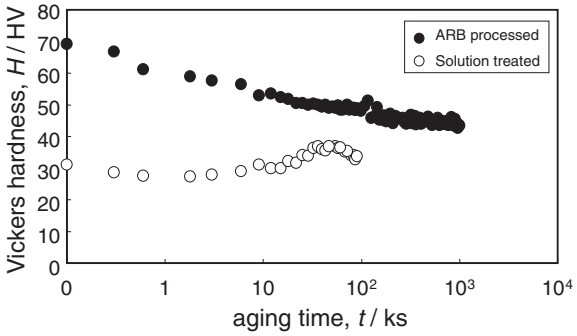

Fig. 2 Variation of Vickers hardness with increasing aging time of ARB-processed and solution-treated specimens aged at 423 K.

the UFGs and measurements of precipitate size were conducted on the {110} plane, where fine Si-phase precipitates were identified. To investigate the inside grain precipitation, selected area electron diffraction (SAED) techniques were used to determine whether Si precipitates existed in the UFGs or grain boundaries.

3. Experimental Results

3.1 The UFG specimen aged at 423 K

Figure 2 presents the micro-Vickers hardness of solution treated specimen and the ARB-processed specimen with UFG at 423 K. The hardness of the solution-treated specimen increased gradually with increasing aging time, reaching the maximum value at an aging time of about 54 ks. The as-ARB-processed specimen has about 2.1 times the hardness of the as-solution-treated specimen. Nevertheless, the hardness of ARB-processed specimens showed no peak of hardness, as the solution-treated specimen and typical precipitation-hardened alloys do. The hardness of the ARB-processed specimen decreased monotonously with increasing aging time from the initial stage of aging to 645 ks. Thereafter, it showed a roughly constant value from 645 ks to 1000 ks. For that reason, we investigated microstructures of ARB-processed specimens aged at 423 K using TEM observations. Figure 3 presents a bright field image and corresponding SAED pattern of as-ARB processed up to a total strain of 4.8 at room temperature. A very fine lamellar boundary structure is readily apparent in Fig. 3(a). Such an elongated lamellar structure is a typical ultrafine microstructure observed in the ARB processed specimen. The mean lamellar boundary width is defined as the mean size of UFG in the present work, and it was about 253 nm. No precipitates exist in the UFG and grain boundaries of the as-ARB processed specimen. An earlier study by Tsuji *et al.* clarified the formation process of UFGs during intense strain (ARB).[1] They also clarified that grain subdivision by sever plastic deformation induced the formation of high-angle boundaries in sub-micrometer scale. The grain boundaries are thought not to contribute to precipitation hardening because almost all lamellar boundaries introduced by severe plastic deformation have high-angle boundaries. Figure 3(b) shows that the SAED pattern in Fig. 3(a) is not spotty but ring-like. Furthermore, no diffraction spots of Si phase are apparent in the SAED pattern. Figures 4(a), (b) and (c) show TEM bright field images of

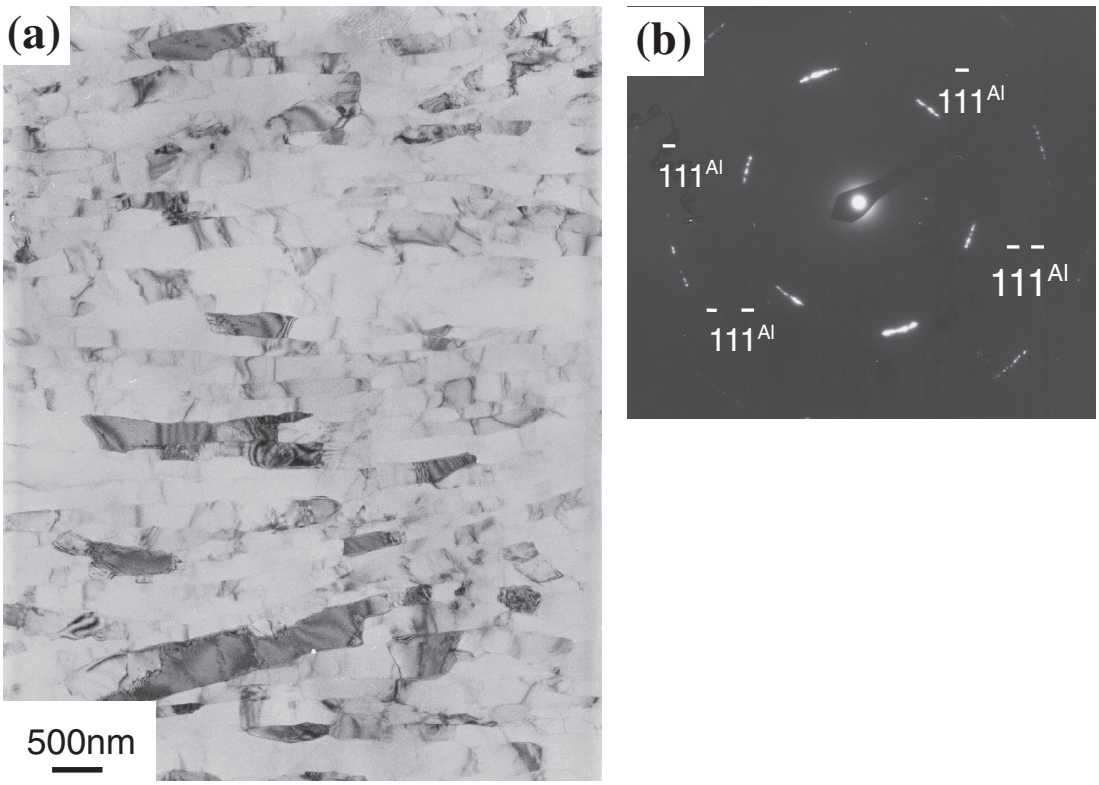

Fig. 3 (a) TEM image for as-ARB processed specimen and (b) its SAED pattern.

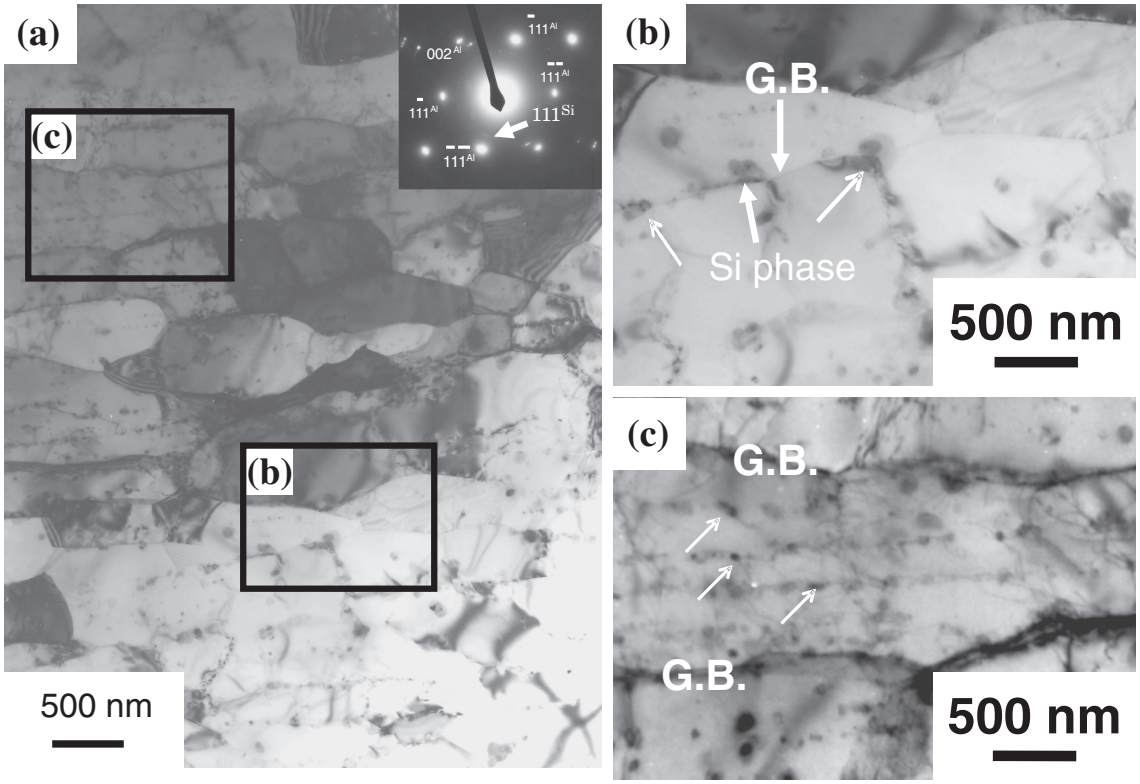

Fig. 4 TEM image and SAED patterns for the specimen aged at 423 K for 1000 ks: (a) low-magnification micrograph. (b) and (c) high-magnification micrographs marked by squares of (b) and (c) in (a).

the specimen aged for 1000 ks at 423 K. Figure 4(b) shows highly magnified images of an area near the grain boundary of (a). In (a), an ultrafine lamellar boundary structure of 633 nm mean size is visible, which is larger than that of as-ARB processed specimen. In the SAED pattern presented in (a), the spots of {111} plane of Si phases are visible. Therefore, the precipitates on the grain boundaries in (a) are identified according to the Si phase. Many lump-shaped

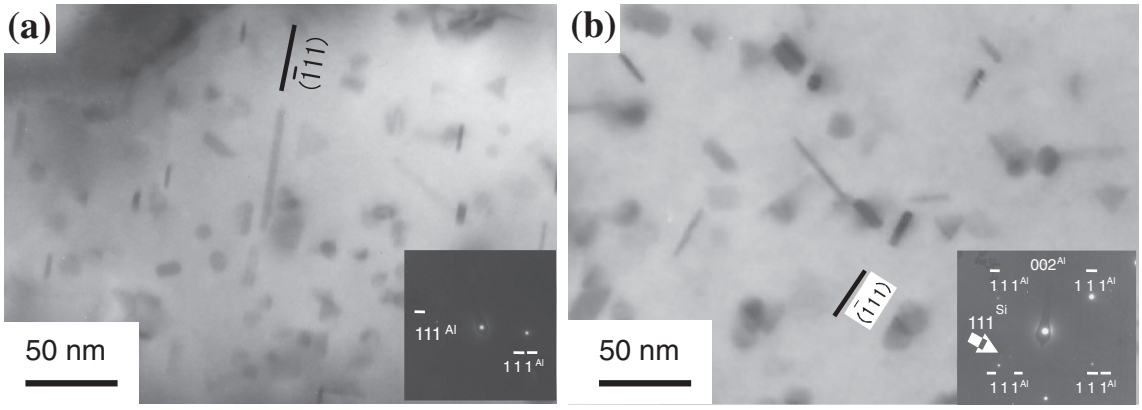

Fig. 5 TEM images and SAED patterns of the ultrafine grain for specimens aged at 423 K for (a) 90 ks and (b) 1000 ks.

precipitates are visible on the grain boundaries in (b). The mean size of the Si phase on the grain boundary is 69.6 nm. However, as shown in Fig. 4(c), many coarse precipitates are arranged linearly in the UFG. The distance between the lines of precipitates is about 250 nm, which is equal to the mean size of the UFG: as-ARB-processed specimen. Therefore, these coarse precipitates are inferred to be Si phase remaining in the UFG after migration of grain boundaries. Moreover, we investigated microstructures in the ultrafine structure of specimens aged at 423 K. Figures 5(a) and (b) present images of the matrix in UFG specimens aged for 90 ks and 1000 ks at 423 K. As these micrographs show, plate-like Si phases precipitate finely on the {111} matrix. The mean size of Si phase in the specimen aged for 90 ks is about 23 nm. The mean size of that in the specimen aged for 1000 ks is about 34 nm. These results show that Si phases in the UFG grow with increasing aging time. Moreover, weak spots in the SAED pattern of the Si phase in specimens aged for 1000 ks were confirmed inside the area of the matrix spots, as shown by a white arrow in Fig. 5(b). Therefore, many nucleation sites for precipitates of Si phase exist in the UFGs. Many solute atoms remain around the Si phase during aging. These Si phase are thought to contribute to precipitation hardening and to restrain grain boundary migration during aging. As described above, the hardness of the UFG specimen aged at 423 K showed a nearly constant value in long-term aging. The authors inferred that precipitation of Si phase in the UFG of the specimen aged at 373 K progresses further than that of the specimen aged at 423 K because the diffusion of solution atoms from the matrix in UFG to grain boundaries of the specimen aged at 373 K is restrained more than that of the specimen aged at 423 K.

3.2 The UFG specimen aged at 373 K

Figure 6 presents a comparison of the variation of Vickers hardness of the UFG specimen with aging times of 373 K and 423 K. The curve at 373 K decreased gradually with increasing aging time from the initial stage of aging to 10 ks, which is similar to the tendency observed for hardness at 423 K. However, the hardness of the specimen aged at 373 K showed a nearly constant value after 10 ks: The rate of decrease of hardness decreased gradually with decreasing aging temperature. Therefore to know the reason, we investigated microstructures of the specimen aged at 373 K using TEM

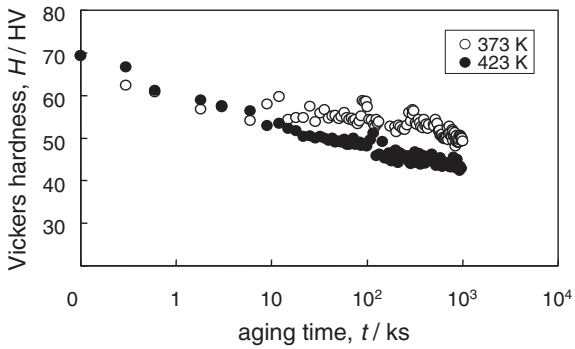

Fig. 6 Variation of Vickers hardness with increasing aging time at 373 K and 423 K.

observation. Figures 7(a) and (b), respectively show a bright field image and SAED pattern of the specimen aged for 1000 ks at 373 K. Figure 7(b) shows a highly magnified image of the area near the grain boundaries as denoted by a white square in (a). The mean size of UFG of the specimen aged for 1000 ks is 453 nm, which is smaller than that of the specimen aged at 423 K for 1000 ks. Moreover, the mean size of Si phase on the grain boundary is 39.5 nm. The size of UFG and Si phase on the grain boundary of the specimen aged at 373 K is smaller than that of the specimen aged at 423 K. Therefore, results show that the mean size of UFG and Si-phase on the grain boundary decreased with decreasing aging temperature. Figure 8 presents microstructural changes in UFGs of specimens aged for 500 ks (a), 800 ks (b), or 1000 ks (c) at 373 K: (a) shows a few small patches (indicated by white arrows) and a plate-like precipitate (indicated by a black arrow). The mean size of all precipitates (black and white arrows) is 7.16 nm. The plate-like precipitate is visible parallel to the {111} plane. Our earlier study revealed plate-like Si phases on the {111} plane that are less than 10 nm at the initial stage of the precipitation process.[7] Therefore it is thought that the plate-like precipitate on the {111} plane in the UFG is Si phase. Moreover, both the mean size of the patch and plate-like precipitate in the specimen aged for 800 ks were 9.71 nm. The small patches and plate-like precipitates are inferred to be Si-phase. In the specimen aged for 1000 ks, they were 9.77 nm. Therefore, the size of precipitates in the UFG increased with increasing aging time at 373 K.

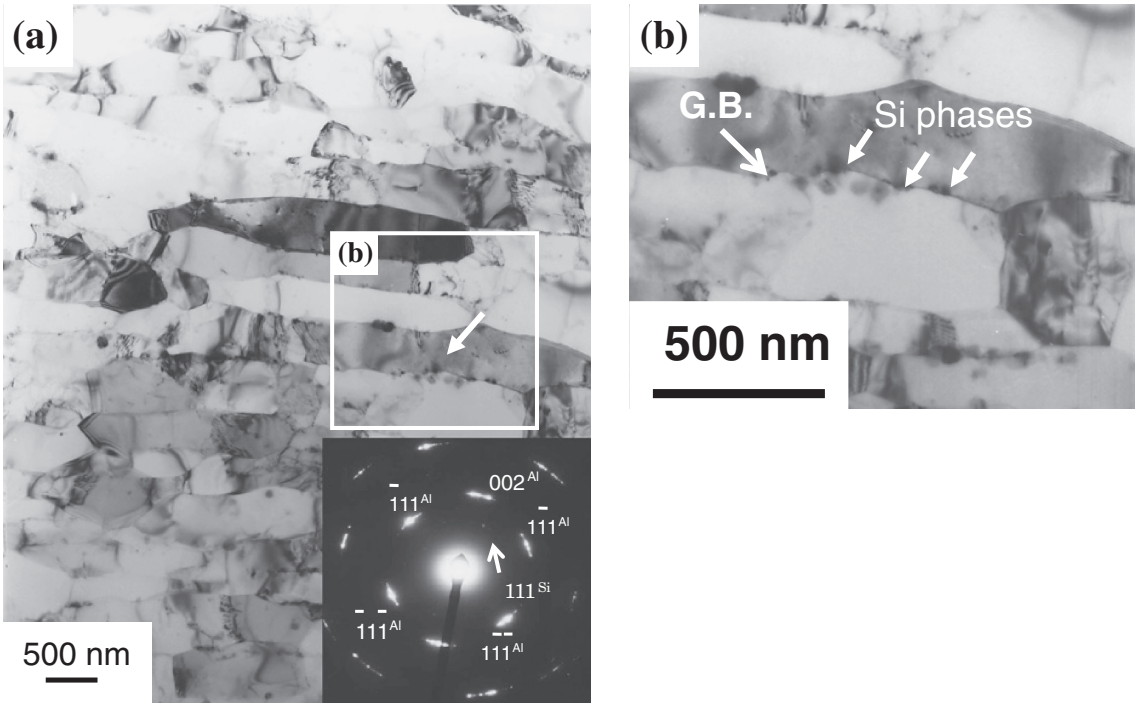

Fig. 7 TEM image and SAED patterns for the specimen aged at 373 K for 1000 ks: (a) low and (b) high-magnification micrographs.

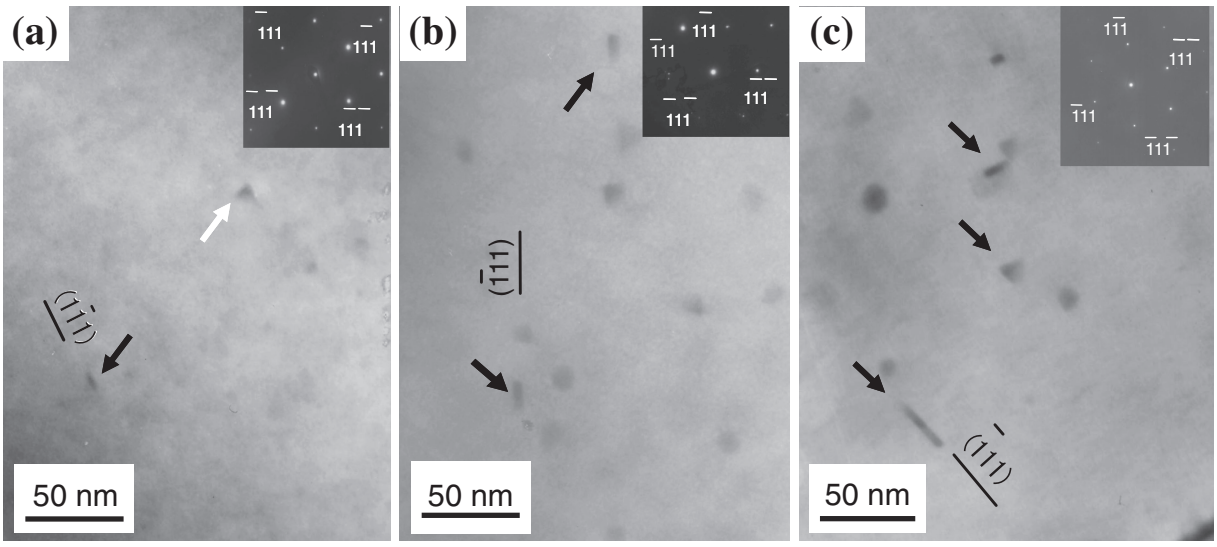

Fig. 8 TEM images and SAED patterns of the ultrafine grain for the specimen aged at 373 K for (a) 500 ks, (b) 800 ks, and (c) 1000 ks.

3.3 Changes of UFG size and aspect ratio

Figures 9(a) and (b) portray changes of the UFG size and aspect ratio in the specimen aged respectively at 373 K and 423 K. As Fig. 9(a) shows, the grain size increases with increasing aging time at each aging temperature. In each curve, an increasing ratio of grain size at the initial stage of aging is larger than at the subsequent aging stage. The ratio of increase of grain size becomes lower with decreasing aging temperature. As (b) shows, the change of the UFG aspect ratio shows an opposite tendency to that of the grain size depicted in panel (a): an increasing ratio of grain size and the decreasing of aspect ratio with decreasing aging temperature. Therefore, it is because the value of hardness decreases with increasing aging time that the mean UFG size increases. The increase of aging temperature is thought to promote the increasing ratio of grain size and decreasing aspect ratio. The discussion presented above implies that increasing grain size and the decreasing aspect ratio decrease hardness with increasing aging time and temperature.

4. Discussion

A lamellar boundary structure was confirmed in the structure of UFGed Al-0.5%Si alloy of as-ARB-processed (Fig. 3). Tsuji *et al.* investigated the mechanism of formation of the lamellar boundary structure, reporting that crystal grains are segmentalized into submicrometer sizes by high-angle boundaries introduced by plastic deformation to form

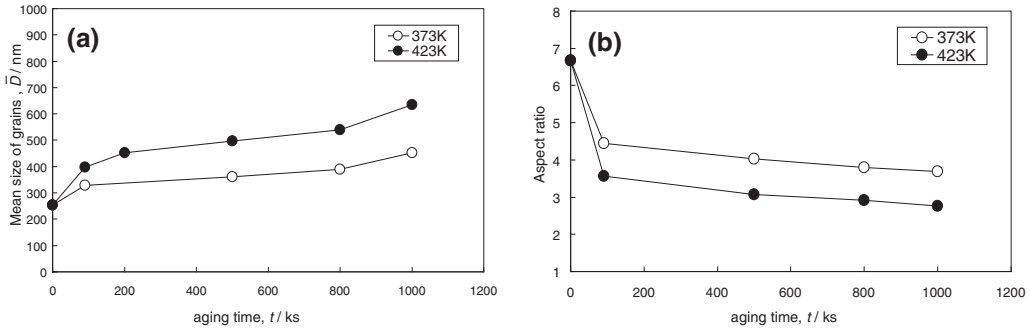

Fig. 9 Variation of mean size and aspect ratio of grains with aging time at 373 K and 423 K: (a) mean grain size and (b) aspect ratio.

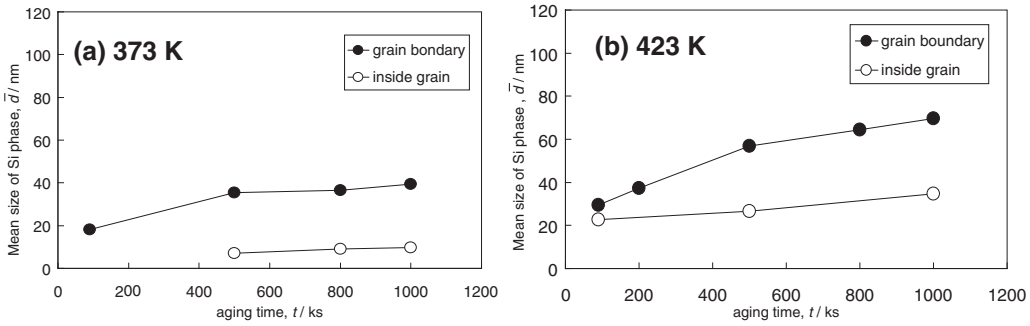

Fig. 10 Variation of mean size of Si phase on inside grains and on grain boundaries with aging time of (a) 373 K and (b) 423 K.

a lamellar boundary (hereinafter, grain boundary) structure. Because a great plastic strain is applied during ARB processing, most grain boundaries formed by deformation produce high-angle boundaries. Furthermore, numerous high-angle boundaries introduced by ARB processing have high interface energy and therefore promote precipitation. As the photograph presented in Fig. 4 shows, many coarse precipitates (Si-phase) are formed in clumps in most grain boundaries. Results of this study clarify that Si-phase in plate-like is precipitated on the {111} plane inside grain in UFGs (Fig. 5 and Fig. 8). However, precipitation of Si-phase in the UFG was less than that at grain boundaries. Figures 10(a) and (b) portray mean size of Si phase on grain boundaries and inside grain with aging time. As shown in this graphs, the mean size of Si-phase precipitated in the grain boundary is greater than those inside grains for aging temperatures 373 K and 423 K. In other words, Si-phase precipitation is known to be faster than that in the UFG, which is regarded as attributable to the fact that many high-angle boundaries exist, and act as preferential precipitation sites for Si-phase precipitation. Therefore, Si-phase precipitation is promoted at the grain boundary. With age hardening, movements of dislocation are normally suppressed by dispersion of microscopic precipitates in grain, thereby strengthening the material. The Si-phase precipitation observed in this study is regarded as contributing slightly to age hardening. As presented in Figs. 2 and 6, reduction in the hardness level by aging might be attributable primarily to softening caused by the recovery and growth of UFGs. Although it is considered that suppression of reduction in the hardness level after many hours of aging is influenced by Si-phase precipitation, details remain unclear. Results of this study also confirmed Si-phase precipitation in the grain after long-term aging at aging temperatures of 423 K or 373 K. This precipitation is regarded as attributable to the fact that, with lower aging temperature, the rate of diffusion of the solute atom (Si-atom) into the grain boundary slows, thereby promoting Si-phase precipitation in the UFG. To assess the possibility of simultaneous pursuit of grain refinement strengthening and age-hardening of the present alloy system, future studies must be conducted to examine effects of various changes in aging temperature and solute atom concentration.

5. Conclusions

We investigated microstructural changes resulting from aging treatment of UFGed Al-0.5%Si alloy fabricated using ARB processes. The following are the main findings:

(1) The mean of grain size of the UFGed Al-0.5%Si alloy produced by the ARB was 253 nm.
(2) The hardness of specimens aged at 373 K and 423 K decreased monotonously with increasing aging time in the initial stage of aging. The hardness value of the specimen aged at 373 K became higher than the value of the specimen aged at 423 K after 10 ks. The rate of decreased of hardness decreased with decreasing aging temperature.
(3) The mean size of the UFG specimen aged at 373 K was less than that of the specimen aged at 423 K.
(4) Si phase precipitated on the {111} planes in the UFG specimen aged at 373 K and 423 K. The mean size of Si-phase in the UFG specimen increased with increasing aging time. The formation of Si phase in the UFG

specimen aged at 373 K is less than that of 423 K in long-term aging.

(5) The formation of Si phases on the grain boundaries is more conspicuous than in ultrafine grains of the specimens aged at 373 K and 423 K.

These results suggest that restraint of the growth of UFG with aging resulted from Si phase precipitates on the grain boundary and lowering of the aging temperature. Moreover the formation of Si-phase in the UFG suggests precipitation hardness in this alloy system.

Acknowledgments

The authors extend their gratitude to Director K. Morishige and Chief Technical Official H. Funamoto, Advanced Instruments Center of Okayama University of Science for assistance during electron microscope observations, and to Professor E. Sukedai and Professor S. Kittaka, Okayama University of Science, for their valuable support. Additionally, we are sincerely grateful to Doctoral Program and Master's Program students of the Tsuji laboratory, Faculty of Engineering, Osaka University, for their assistance during ARB processing.

REFERENCES

1) N. Tsuji, Y. Saito, S. H. Lee and Y. Minamino: Adv. Eng. Mater. **5** (2003) 338–344.
2) N. Tsuji, T. Iwata, M. Sato, S. Fujimoto and Y. Minamino: Sci. Technol. Adv. Mater. **5** (2004) 173–180.
3) Z. Horita, K. Ohashi, T. Fujita, K. Kaneko and T. G. Langdon: Adv. Mater. **17** (2005) 1599–1602.
4) H. S. Rosenbaum and D. Turnbull: Acta Metall. **6** (1958) 653–659.
5) H. S. Rosenbaum and D. Turnbull: Acta Metall. **7** (1959) 664–674.
6) A. Saulnier: Mem. Sci. Rev. Met. **58** (1961) 615–625.
7) K. Nakagawa, T. Kanadani, L. Anthony and H. Hashimoto: Mater. Trans. **46** (2005) 779–783.